Colloidal particle deposition in porous media under flow: A numerical approach

Yajie Li, Otar Sarishvili, Aziz Omari, Azita Ahmadi, and Hongting Pu

***Abstract* — The objective of this study is to simulate the transport and deposition of colloidal particles at the pore scale by means of computational fluid dynamics simulations (CFD). This consists in the three-dimensional numerical modeling of the process of transport and deposition of colloidal particles in a porous medium idealized as a bundle of capillaries of circular cross section. The velocity field obtained by solving the Stokes and continuity equations is superimposed to particles diffusion and particles are let to adsorb when they closely approach the solid wall. Once a particle is adsorbed the flow velocity field is updated before a new particle is injected. Our results show that both adsorption probability and surface coverage are decreasing functions of the particle's Péclet number. At low Péclet number values when diffusion is dominant the surface coverage is shown to approach the Random Sequential Adsorption value while it drops noticeably for high Péclet number values. Obtained data were also used to calculate the loss of porosity and permeability.**

***Index Terms* — porous media, particle transport, deposition, pore scale numerical simulation.**

I. Introduction

Porous media are of scientific and technological interest because of the wide spectrum of applications they have attained during the past decades [1]. Various methods have been used for the design of porous media, such as foaming process, template technique, sol-gel, hydrothermal synthesis, precipitation, chemical etching methods and photolithographic techniques [2-7]. Several types of porous media including porous polymers, organic-inorganic hybrid porous materials, and porous carbon aerogels have been successfully synthesized in our previous works [8-10]. These porous materials are used for many purposes, namely for water filtration and waste water treatment which are the focus of this study.

Moreover, particle transport and deposition processes in porous media are of great technological and industrial interest since they are useful in many engineering applications and fundamentals [11-13] including contaminant dissemination, filtration, chromatographic separation and remediation processes [14-19]. To characterize these processes, numerical simulations have become increasingly attractive due to growing computer capacity and calculation facilities offering an interesting alternative, especially to complex in situ experiments [20-22]. Basically, there are two types of simulation methods, namely macro-scale simulations and micro-scale (pore scale) simulations. Macro-scale simulations describe the overall behavior of the transport and deposition process by solving a set of differential equations that gives spatial and temporal variation of particles concentration in the porous sample without providing any information regarding the nature or mechanism of the retention process [17]. Micro-scale (pore scale) numerical simulations directly solve the Navier-Stokes or Stokes equation to compute the flow and model particle diffusion processes by random walk for example [23].

The objective of the current work is to simulate the process of particles transport and deposition in porous media at the pore scale by means of CFD simulations in an easy way in order to get the most relevant quantities by capturing the physics underlying the process.

II. Method and Tools

A. Method

The present work focuses on three-dimensional numerical modeling of the process of transport of particles in a pipe as porous media are usually represented as a bundle of capillaries. This is done by coupling two available soft wares. First, the velocity field is obtained by solving the Stokes and continuity equations by means of the popular OpenFOAM® (Open Field Operation and Manipulation) shareware and secondly particle's tracking is performed with Python® software [24]. No-slip boundary condition is applied on the pore wall, and the pressure at the inlet and outlet are set to fixed values.

The particle-pore wall interaction is considered purely attractive while particle-particle interaction is purely repulsive. Particles are injected sequentially at a random initial position at the inlet of the pipe and their center of mass is tracked until either they reach the outlet of the domain or are deposited onto the pipe surface. The particles' mean diameter and flow conditions are chosen in a way that the particle's Reynolds number is sufficiently small so that the particles can be treated as a mass point. However, once a

Manuscript received December 15, 2016. This work was supported in part by the I2M, TREFLE Department, France, and the scholarship from China Scholarship Council (CSC) under the Grant CSC N° 201506260062.

Y. J. Li is with the School of Materials Science and Engineering, Tongji University, China, and I2M, TREFLE Department, France. (e-mail: yajie.li@ensam.eu).

O. Sarishvili is with I2M, TREFLE Department, France. (e-mail: osarishvili@googlemail.com).

A. Omari is with I2M, TREFLE Department, France. (e-mail: omari@enscbp.fr).

A. Ahmadi is with I2M, TREFLE Department, France. (e-mail: a.ahmadi@i2m.u-bordeaux1.fr).

H. T. Pu is with the School of Materials Science and Engineering, Tongji University. (e-mail: puhongting@tongji.edu.cn).

particle is deposited, an equivalent volume surrounding the deposition location is set to be solid on the pore surface. Then the new velocity field is recalculated to take into account the influence of the presence of the deposited particle on the flow and a new particle is then injected. The injection process is repeated until particle deposition probability vanishes.

B. Determining the Flow Field in OpenFOAM Shareware

The hydrodynamic model is solved with OpenFOAM package, which is a versatile equations' solver and can be used to solve different kinds of differential equations. It should be noticed that the hydrodynamic model is used to generate input flow data for the particle transport model.

C. Lagrangian Particle Tracking in Python®

Injected particles are tracked using a Lagrangian method. Three situations may occurs: (i) the particle is adsorbed onto the solid wall when it approaches it closely if a free surface is available for deposition; (ii) the particle leaves the domain and never comes close to the wall surface; (iii) the particle comes close to the solid surface but the deposition site is occupied by another particle repealing it to the bulk flow. The velocity at every node is the vector summation of the interpolated convection velocity $\mathbf{V_{int}}$ (obtained from OpenFOAM) and the Brownian diffusion velocity $\mathbf{V_{diff}}$:

$$\mathbf{V} = \mathbf{V_{int}} + \mathbf{V_{diff}} \tag{1}$$

where $\mathbf{V_{int}}$ is the flow velocity computed at a given position by interpolating the velocity values calculated by the hydrodynamic model for the eight surrounding nodes. The stochastic movement of the particles is realized through the calculation of $\mathbf{V_{diff}}$ at every position knowing its diffusivity coefficient, D, given by

$$D = \frac{k\,T}{6\pi\,\mu\,a} \tag{2}$$

where k is the Boltzmann constant, T the absolute temperature, μ the dynamic viscosity of the suspending fluid and a the particle radius. The diffusion velocity $\mathbf{V_{diff}}$ is related to the diffusion coefficient D through the following relationship:

$$\mathbf{V_{diff}} = \sqrt{\frac{D}{t_r}} \tag{3}$$

where t_r is the referential time [24],

$$t_r = \zeta / (2\, u_{max}) \tag{4}$$

In Eq. (4); ζ stands for the characteristic mesh size and u_{max} is the maximum of actual velocity along the mean flow axis. New positions of the moving particle are obtained by summing the old position vector and the sum of the diffusion velocity and the convection velocity multiplied by the referential time [24]:

$$\mathbf{X}_{new} = \mathbf{X}_{old} + \mathbf{V}\ tr \tag{5}$$

D. Simulation parameters

The parameters used in the simulations are summarized in table I below.

TABLE I: DETAILED PARAMETERS OF THE SIMULATION

Parameters	**Values**
Particle diameter, a (m)	$4\ 10^{-7}$
Pipe length, L (m)	$1.5\ 10^{-5}$
Pipe radius, R (m)	$4\ 10^{-6}$
Pressure drop, Δp (Pa)	From 10^{-5} to 1
Péclet number, Pe	From 0.0015 to 150
Boltzmann constant, k (J/°K)	$1.38\ 10^{-23}$
Temperature, T (°K)	293.15
Diffusion coefficient, D (m^2/s)	$5\ 10^{-11}$
Dynamic viscosity, μ (Pa s)	10^{-3}

Following a sensitivity analysis, for all simulations a mesh number of 50 × 50 × 40 is chosen with a mesh refinement in the vicinity of solid walls.

The Péclet number (Pe) is a dimensionless number that is relevant for the study of transport phenomena of colloidal dispersions. Here, it is defined to be the ratio of the rate of advection to the rate of particle's diffusion:

$$Pe = \frac{u_{average} a}{D} \tag{6}$$

where $u_{average}$ is the average convection velocity along the mean flow axis.

III. RESULTS AND DISCUSSION

A. Deposition probability

Fig. 1 shows the variation of the deposition probability versus the number of injected particles for different Péclet numbers ranging from low Pe where diffusion is dominant to high Pe where the transport is mainly governed by convection. The probability of deposition is defined as the ratio of the deposited particles over the injected particles and is calculated over groups of 200 injected particles.

For the diffusion-dominant regime at low Péclet number, the deposition probability is high for a small number of injected particles and decreases slowly as more particles are injected. This is due to the fact that for a lower number of injected particles, the wall surface is free and the injected particles easily find a place to deposit. When the number of adsorbed particles reaches a certain value, the deposition probability drops sharply to reach lower values for higher numbers of injected particles. When this sharp transition is approached, the surface wall is already covered by many adsorbed particles and further injected particles will have much less probability to deposit. For high Péclet numbers, where the transport is dominated by convection, the available surface for adsorption is potentially lower that for the diffusion dominant regime. Indeed, there is a larger exclusion surface around already deposited particles due to hydrodynamic shadowing effect. This leads to lower values for the deposition probability [24].

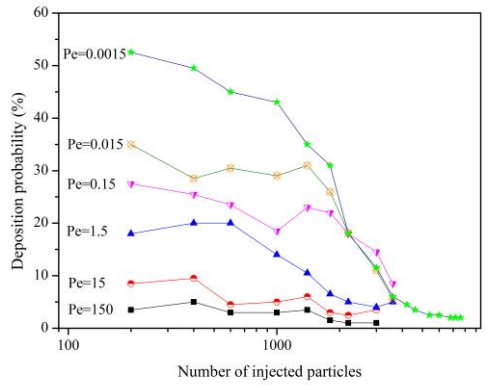

Fig. 1. Variation of deposition probability versus the number of injected particles for different Péclet numbers.

B. Surface coverage

Surface coverage (Γ) is defined as the ratio of the total projection area of the deposited particles to the pipe surface area. Moreover, it is well known that for pure diffusion regime and a flat surface using the Random Sequential Adsorption (RSA) model, the maximum surface coverage, Γ_{RSA}, is found to be close to 0.546 [24, 25]. The surface coverage Γ is therefore made dimensionless using this value.

The dependency of Γ/Γ_{RSA} on the number of injected particles for different Péclet numbers is shown in Fig. 2. As expected, the surface coverage increases with the number of injected particles and it decreases with the Péclet number. For the most diffusive case considered here, Pe = 0.0015, the dimensionless surface coverage reaches values close to $0.8\Gamma_{RSA}$, while for the large Peclet number, Pe = 150, corresponding to a fully convection-dominant regime, Γ/Γ_{RSA} is as low as 0.05. We must recall that the surface coverage is an important parameter because it is linked to the performance of the porous medium when it is used for water filtration for solid particles or micro-organisms removal. For these applications, a high value of surface coverage is therefore aimed.

In Fig. 3, the geometry and the adsorbed particles are presented after the injection of 3000 particles for the two extreme Pe numbers (Pe=0.0015 and Pe=150). As it can be seen, for higher Pe, the number of deposited particles is much less than that obtained for lower Pe, which is a visual illustration of the analysis is made above.

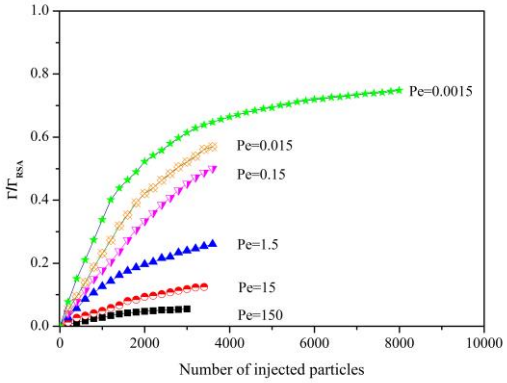

Fig. 2. Variation of Γ/Γ_{RSA} versus the Péclet number.

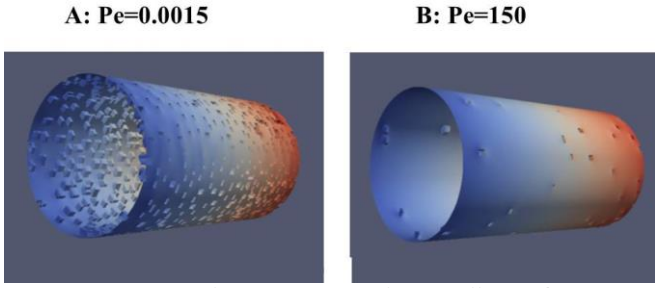

Fig. 3. Visual illustration of adsorbed particles for two different Péclet numbers after the injection of 3000 particles (A) Pe=0.0015 and (B) Pe=150.

C. Porosity and permeability reduction

In processes such as water reinjection in enhanced oil recovery technics, colloids transport and namely particle deposition has an important role in porous media damage and water injectivity decline, since deposited particles influence the petrophysical properties of the reservoir namely the porosity and the permeability. The variations of these properties versus the number of the injected particles are plotted in Fig. 4 and 5.

Here, the porosity is defined as the ratio of the pore volume after deposition and the overall initial pipe volume. As expected, for different Péclet numbers, the porosity decreases with the number of injected particles. The porosity reduction trend is faster for smaller Péclet numbers as a consequence of mecanisms discussed previously and the final porosity decreases with the Péclet number as well.

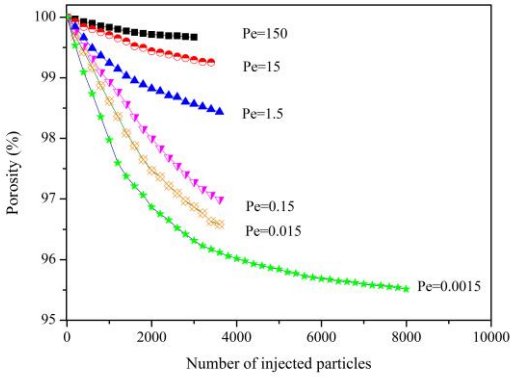

Fig. 4. Porosity versus the number of injected particles at various Péclet numbers.

In this study, the permeability is calculated by:

$$K = \frac{u_{average}\ \mu L \phi}{\Delta p} \qquad (6)$$

where $u_{average}$ is the average convection velocity along the mean flow axis, μ is the dynamic viscosity of the injected fluid, L is the length of the pipe, ϕ is the porosity of the pipe, and Δp is the pressure drop between the inlet and the outlet face. The permeability reduction factor, R_k is defined as the ratio of K to K_Γ where K and K_Γ stand for the permeability before and after deposition. K is constant for all Pe and equal to 1.51×10^{-12} m^2. The variation of R_k versus the number of injected particles is plotted in Fig. 6 for each value of Pe. The permeability decreases with the number of injected particles, and the trend is more pronounced for diffusion dominant regimes (smaller Péclet numbers). Knowing the R_k values, one can estimate the hydrodynamic thickness of deposited layer δ using Poiseuille's law:

$$\frac{\delta}{R} = 1 - R_k^{-1/4} \quad (7)$$

Therefore, for the lowest Pe considered here, from the plateau value of R_k, a thickness δ to be compared to the particle diameter (δ=340 nm versus 2a=800 nm) demonstrating the formation of a loose mono-layer deposit. For Pe = 150, δ decreases down to around 100 nm.

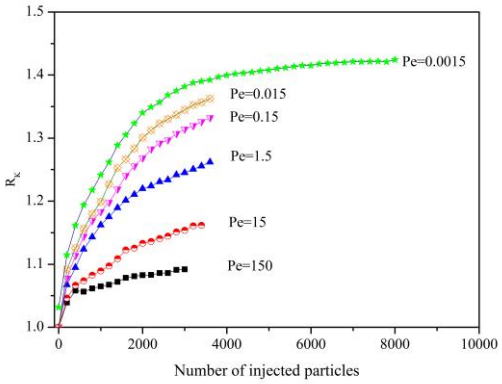

Fig. 5. Variation of permeability reduction versus the number of injected particles at various Péclet numbers.

IV. Conclusions

Numerical simulations of the deposition of colloidal particles onto porous media of simple geometry under flow have been carried out. Preliminary results were analyzed and the some conclusions may be drawn. The deposition probability decreases with the number of the injected particle and with the Péclet number. At low Péclet number values, the surface coverage Γ is shown to closely approach the RSA value and it drops noticeably for high Pe values. Both the porosity and the permeability decrease with the number of deposited particles. At lower Pe numbers, the final hydrodynamic thickness of the deposit layer is lower than the particle diameter showing the formation of a loose monolayer deposit and it decreases for higher Pe. The above results, though they need to be consolidated, are consistent with theoretical predictions, demonstrating that the numerical method used is relevant to describe deposition of colloids in porous media from dilute dispersions. Future developments of this work will include a larger range of the related parameters on the one hand and more realistic pore geometries on the other hand.

V. Acknowledgment

This work was supported in part by the China Scholarship Council (CSC) under the Grant CSC N° 201506260062.

References

[1] F. A. Coutelieris, and J. M. P. Q. Delgado, "Transport Processes in Porous Media. Advanced structured materials," *Springer Berlin Heidelberg*, 2012.

[2] Z. H. Li, C. Cheng, X.Y. Zhan, Y. P. Wu, and X.D. Zhou. "A foaming process to prepare porous polymer membrane for lithium ion batteries," *Electrochimica Acta*, vol. 54, no. 18, pp. 4403-4407, 2009.

[3] S. A. Johnson, P. J. Ollivier, and T. E. Mallouk. "Ordered mesoporous polymers of tunable pore size from colloidal silica templates," *Science*, vol. 283, no. 5404, pp. 963-965, 1999.

[4] M. Gaberscek, M. Remskar, D. Hanzel, J. M. Goupil, S. Pejovnik, R. Dominko, M. Bele, and J. Jamnik, "Porous olivine composites synthesized by solgel technique," *Journal of Power Sources*, vol. 153, no. 2, pp. 274-280, 2006.

[5] M. Zawadzki, and J. Wrzyszcz, "Hydrothermal synthesis of nanoporous zinc aluminate with high surface area," *Materials Research Bulletin*, vol. 35, no. 1, pp. 109-114, 2000.

[6] M. Hernandez-Guerrero, and M. H. Stenzel, "Honeycomb structured polymer films via breath figures," *Polym. Chem.*, vol. 3, pp. 563-577, 2012.

[7] U. Welp, H. H. Wang, W. K. Kwok, G. A. Willing, J. M. Hiller, R. E. Cook, D. J. Miller, Z. L. Xiao, C. Y. Han and G. W. Crabtree, "Fabrication of alumina nanotubes and nanowires by etching porous alumina membranes," *Nano Letters*, vol. 2, no. 2, pp. 1293-1297, 2002.

[8] Y. J. Li, X. Y. NI, J. SHEN, D. Liu, and N. P. Liu, "Preparation and performance of polypyrrole/nitric acid activated carbon aerogel nanocomposite materials for supercapacitors," *Acta Phys Chim Sin*, vol. 32, no.2, pp. 493-502, 2016.

[9] Y. J. Li, X. Y. NI, J. SHEN, D. Liu, and N. P. Liu, "Polypyrrole/nitrate activated carbon aerogel composite materials for supercapacitors," *Journal of Functional Materials*, vol. 12, no.44, pp. 1750-1754, 2013.

[10] H. T. Pu, and Y. J. Li, "a porous styrenic material for the adsorption of polycyclic aromatic hydrocarbons," Chinese patent 201510812566.9.

[11] G. Qiu, J. Xiao, and J. Zhu, "Research history, classification and applications of metal porous material," *Metalurgia International*, Vol. 18, no. 5, 2013.

[12] M. Y. Corapcioglu, and S. Jiang, "Colloid-facilitated groundwater contaminant transport," *Water Resources Research*, Vol. 29, no. 7, pp. 2215-2226, 1993.

[13] J. M. P. Q. Delgado, "Industrial and technological applications of transport in porous materials," *Springer*, 2013.

[14] N. Sefrioui, A. Ahmadi, A. Omari, and H. Bertin, "Numerical simulation of retention and release of colloids in porous media at the pore scale," *Colloids and Surfaces A: Physicochemical and Engineering Aspects*, vol. 427, pp. 33-40, 2013.

[15] N. Sefrioui, A. Ahmadi-Senichault, H. Bertin, and A. Omari, "On the influence of ionic strength on colloid transport in porous media in the presence of a rough surface: numerical simulation at the microscopic scale," *Colloids and Complex Fluids: Challenges and Opportunities*, 17-19 October 2012, IFP Energies nouvelles, Rueil-Malmaison (France).

[16] A. Scozzari, and B. E. Mansouri, "Water security in the mediterranean region: an international evaluation of management, control, and governance approaches," *NATO science for peace and security series C: environmental security*. Springer Netherlands, 2011.

[17] G. Boccardo, D. L. Marchisio, and R. Sethi, "Microscale simulation of particle deposition in porous media," *Journal of Colloid and Interface Science*, vol. 417, pp. 227-237, 2014.

[18] S. Khirevich, A. Höltzel, A. Daneyko, A. Seidel-Morgenstern, and U. Tallarek, "Structure–transport correlation for the diffusive tortuosity of bulk, monodisperse, random sphere packings," *Journal of Chromatography A*, vol. 1218, pp. 6489-6497, 2011.

[19] T. Tosco, J. Bosch, R. U. Meckenstock, and R. Sethi, "Transport of Ferrihydrite Nanoparticles in Saturated Porous Media: Role of Ionic Strength and Flow Rate," *Environmental Science & Technology*, vol. 46, no. 7, pp. 4008-4015.

[20] D. L. Marchisio, G. Boccardo, and R. Sethi, "Microscale simulation of particle deposition in porous media," *Journal of Colloid and Interface Science*, vol. 417, pp. 227-237, 2014.

[21] J. Serlemitsos, E. Liu, A. H. Reed, W. Long, H. Huang, and M. Hilpert, "Pore-scale study of the collector efficiency of nanoparticles in packings of nonspherical collectors," *Colloids and Surfaces A: Physicochemical and Engineering Aspects*, vol. 358, no. 13, pp. 163-171, 2010.

[22] W. Long, and M. Hilpert, "A correlation for the collector efficiency of brownian particles in clean-bed filtration in sphere packings by a lattice-boltzmann method," *Environmental Science & Technology*, vol. 43, no. 12, pp. 4419-4424, 2009.

[23] F. Xiao, "Pore-scale Simulation Frameworks for Flow and Transport in Complex Porous Media," PhD thesis, Department of Petroleum Engineering, Colorado School of Mines. 2013.

[24] P. Lopez, A. Omari, and G. Chauveteau, "Simulation of surface deposition of colloidal spheres under flow," *Colloids and Surfaces A: Physicochemical and Engineering Aspects*, Vol. 240, no. 1, pp. 1-8, 2004.

[25] J. Talbot, G. Tarjus, P. R. Van Tassel, and P. Viot, "From car parking to protein adsorption: an overview of sequential adsorption processes," *Colloids and Surfaces A: Physicochemical and Engineering Aspects*, Vol. 165, pp. 287-324, 2000.